

*November 1987**NIKHEF-H/87-21***STRAIGHT LINE CALIBRATION IN
DRIFT CHAMBERS OVER EIGHT METERS***Fred HARTJES¹, Jan KONIJN² and Yue PENG**NIKHEF-H, Amsterdam, The Netherlands**P.O. Box 41882, 1009 DB***Abstract**

Results are presented from a feasibility study of the use of UV Nitrogen lasers for the alignment of a large system of stacked drift chambers. They prove that a straight line calibration is possible over a distance of eight meters with deviations of less than 10 μm . The results could be reproduced by a computer simulation.

¹ Contact Person

² Now at Philips, Eindhoven, The Netherlands

1. Introduction

Alignment of drift chamber systems over large distances has become a necessary requirement for obtaining high accuracy in large particle detectors. Ionisation tracks produced by a UV laser beam are particularly suited for this purpose as the laser beam itself is unperturbed by magnetic fields and can be spatially controlled with very high precision [1-2].

In a previous paper [3] a four meter long straight calibration line generated by a laser was proven to be possible. In one of the applications, the L3 muon chamber system, even longer beams of up to eight meters are necessary. A straightforward extrapolation of the technique described in reference [3] turned out not to give the required accuracy of less than 20 μm .

In this article, we first describe an alternative optical system which enables a laser calibration within the desired tolerances over such large distances. Secondly we present the results of a simulation model which takes into account the various aspects of the interaction of the laser beam with a drift chamber and its electronics. A surprisingly good agreement was found for the pulse shapes, the variation along the beam of the ionisation and the drift time measurements.

2. Experimental set up

Figure 1 shows the test set up including the laser, optical system and the drift chamber used for this investigation. The home built Nitrogen laser (fig. 2) emitted 50 μJ pulses of 0.8 ns at 337 nm. The beam had a Gaussian shape in the direction perpendicular to the laser plates (corresponding to the drift direction in the chamber). The beam divergence was mainly limited by diffraction. Changing the laser repetition rate from 1 to 5 Hz caused a small increase in the beam width parallel to the laser plates. This effect could be compensated by readjusting the distance between the cylindrical lenses CL1 and CL2 in fig. 2.

In this set up the laser beam profile can be regulated in the following ways:

1. By adjusting the distance between the lenses C1 and C2 of the beam width adapter (BWA) the beam focal point can be controlled.
2. By changing the ratio of the focal length of the two BWA lenses, the beam diameter can be controlled.
3. By reducing the diaphragm opening D , the tails of the beam profile distribution and the spurious light can be cut off. As a consequence however, interference phenomena are invoked which appear to be

crucial for the straight line calibration.

The drift chamber used was a test model for the L3 muon chambers {5} using 5.4 m long gold plated tungsten ($\varnothing = 20 \mu\text{m}$) sense wires. The wires were connected to fast pre-amplifiers³, followed by low slew leading edge discriminators. The chamber was operated with an Argon - ethane mixture in a ratio of 61:39. About 60 ppM of N,N-diethylaniline was added to provide a stable laser ionisation. For this admixture the relation between the number of liberated electrons per unit of length (n_e) and light intensity (I) for the wavelength of the Nitrogen laser (337 nm) is given by {6}:

$$n_e \sim I^2 \quad (1)$$

Most measurements were done at a voltage setting for which the electric field in the drift region was calculated to be 8.25 V/cm. The drift velocity for this electric field value was assumed to be 51.5 $\mu\text{m/ns}$, based on previous measurements {5}.

As it was not possible to use an optical bench with the required straightness and length (<10 μm resp. 5 m), the sum of the drift times from both sides of the wire plane was observed. Using mirror assembly B, mounted on a precision stage (see fig. 1), measurements of the drift times T1 and T2 at the positions 1 and 2 respectively were taken, each averaged over 100 laser shots. The distance between position 1 and 2 was reproducible to a few micrometers.

The mirror assembly A was set at various positions along an optical bench and for each of these positions a corresponding drift time sum (T1+T2) was calculated. Note that (T1 + T2) is not affected by possible errors in the optical bench. In this way positions along the 10 m long laser beam were scanned. (T1 + T2) was corrected for the propagation time of the laser light to the drift chamber.

A linear relation between the mirror assembly A position and the drift time sum (T1 + T2) implies that laser induced events can be used to simulate straight particle tracks in a system of drift chambers, under the assumption that the laser beam is symmetric. The calibration line obtained from the drift time sum measurements is not necessarily parallel to the line passing through the center of the laser beam since the beam profile is not the same over its full length. The correctness of the linear relation and its dependence on the various settings of the optical system, the threshold level of the discriminator and the sense wire electronic parameters will be described in the next section.

3. Results

The experiment started by taking measurements with optical settings similar to the ones described in reference {3}. In that case the beam was focused on a point 6 m away from the diaphragm D so that a useful calibration line of 4 m was obtained. The diameter of the beam at the BWA was equal to the diameter at the focus. As a consequence a waist having higher ionisation is formed between the diaphragm and the focal point {4}. The diaphragm did not cut off the beam for the settings used. In order to get an 8 m long useful calibration line the optical parameters were scaled. The results turned out to be unsatisfactory as can be seen in fig. 3, where the drift time sum (T_1+T_2) of one sense wire is plotted as a function of the optical distance (X) between the sense wire and the BWA. No straight line within the the required tolerance of $10 \mu\text{m}$ could be drawn through the measured events.

The situation could be improved after systematic investigation of the three parameters of the beam shaping optics as described in section 2, leading to substantially different settings from the ones described in reference {3}. The optical setting with the best result appeared to be:

1. a beam width at the BWA of $\sigma = 1.04 \pm 0.10$ mm, the beam profile being described by a Gaussian:

$$I(r) = I_0 \cdot \exp(-r^2/2 l^2) \quad (2)$$

where $I(r)$ is the light intensity at a distance r from the centre of the beam.

2. a focus between infinity and $f = -75$ m, which means a slightly diverging beam.
3. a diaphragm opening with a diameter of 3.6 mm. As a result the edges of the beam were cut off at $|r| = 1.8$ mm and diffraction patterns could be observed.

In fig. 4 an example of the measurement of (T_1+T_2) as a function of X is shown. Numerous measurements of (T_1+T_2) as a function of X were taken under these optical conditions for various values of the ratio of the voltage of the sense wire pulse ($V_{c,h}$) and the threshold setting of the discriminator ($V_{t,h}$). For all measurements straight lines were fitted between $X=2$ m and $X=10$ m. The RMS distance to the calibration line was used as an indication of its straightness. In fig. 5 the RMS deviation is plotted as a function of the ratio $V_{c,h}/V_{t,h}$. The figure shows that for values of $V_{c,h}/V_{t,h}$ greater than 4 the deviation from a straight line is smaller than $10 \mu\text{m}$.

Several checks were made to investigate the sensitivity and reproducibility of the results. The optical parameters were slightly varied, the measurements were several times repeated, but the results only varied within the expected error region.

The straightness of the calibration line was also studied for laser beams which were not parallel to the sense wire plane. An angle of incidence of 4° with respect to this plane was chosen, corresponding to a time shift of 14 ns from one wire to another. As the avalanche induced crosstalk was rather high (12%), the pulse height in the leading edge of the sense wire pulse is reduced. This results in an increased drift time. However, no significant effect on the straightness of the calibration line could be observed.

For the laser beam energy of 8.5 to 10 μJ used in these measurements, the ionisation in the chamber was found to be of the order of 150 ion pairs per cm. In fig. 7 the ionisation measured as a function of X is shown. A slight decrease for high values of X can be observed for a diaphragm opening of 3.6 mm and a focus at $f = -75$ m. This is in contradiction with the rapid decrease expected due to the beam divergence. Apparently the decrease is compensated by enhancement from the diaphragm induced interference patterns.

4. Model calculation

A computer program was written to simulate the response of the drift chamber to the laser beam. The simulation includes the calculation of the laser beam profile, the generation of the ion clouds, the influence of the drift path differences near the sense wire on the pulse shape, the broadening by diffusion of the electron cloud and the effect of the electrical wire characteristics.

The beam profile, which is influenced by the diaphragm cutoff, can be described by the Fresnel diffraction theory {8}. For its computation the Huygens-Fresnel principle of imaginary oscillators was used. A numerical approach was chosen as the analytical solution was difficult to evaluate. The calculation started from a rectangular grid of light sources on a circular area (the diaphragm), the intensity distribution was given by a Gaussian(2); the experimental parameters for the beam shaping optics were used. The curved wave front of a focused beam was simulated by introducing phase shifts depending on r . The profile along the beam was found by adding for each point the contributions of the light sources on the diaphragm surface. Using the relation (1) the ionisation distribution was obtained.

The sense wire signal was assumed to be proportional with the flux of primary electrons. Each electron was supposed to yield a Gaussian shaped

pulse with a σ of 10 ns. This is certainly a good approximation for the first part of the rising edge of the sense wire pulse where the influence of the ion space charge is still small. It is this part that triggers the leading edge discriminator. The time dependence of the signal was found by integrating slices of the laser induced ionisation track for each possible drift path. The time difference between the various drift paths was experimentally obtained for this drift chamber using a strongly focused laser beam as described in reference {7}.

The effect of longitudinal diffusion was calculated by a convolution of the signal shape with the Gaussian diffusion function. The σ of this function was found from:

$$\sigma_D = \sigma_I \times \sqrt{Y} / v_D \quad (3)$$

where σ_I is the diffusion parameter of $180 \mu\text{m}/\sqrt{\text{cm}}$, Y the drift distance in cm, and v_D the drift velocity of $51.5 \mu\text{m}/\text{ns}$.

The dispersion of the pulse when propagating along the sense wire was taken into account by considering the wire as a number of RLC networks. For R the value of $270 \Omega/\text{m}$ was used, a result of the calculation of the Ohmic wire resistance at the skin depth at 300 Mhz. For C the measured value of $14 \text{ pF}/\text{m}$ was taken. The value for L of $1.4 \mu\text{H}/\text{m}$ was found from $v = 1/\sqrt{LC}$ by estimating the phase velocity v at $2.25 \times 10^8 \text{ m/s}$. The RC broadening of the preamplifier with a time constant of 1.36 ns was also included in the model.

Fig. 6 shows the comparison between a set of measured drift time sums and the corresponding calculated ones. The calculation does not only give a straight calibration line, but its slope and further characteristics correspond well with the measurements. The largest difference corresponds to a distance of $20 \mu\text{m}$.

In fig. 7 the calculated and observed ionisation are compared as a function of X. Here too the correspondence between calculation and measurement is surprisingly good. The rapid decrease of the ionisation calculated for a beam without diaphragm indicates the importance of this optical element.

As a third and last check for the correctness of the model the rising edge shape of the drift chamber pulse was calculated. Experimentally, the shape can be determined by measuring the drift time for various values of V_{ch}/V_{th} . Fig. 8 shows this dependence which is nothing else but a logarithmic display of the pulse shape. Again a nice correspondence between calculation and measurement is found. Starting at $V_{ch}/V_{th} = 3$ the dependence is almost a straight line, with a slope corresponding to $43 \mu\text{m}/\text{dB}$. This means that a large part of the rising edge can be approximated by an exponential shape. The slow rise of the laser induced pulse compared with the value of about $10 \mu\text{m}/\text{dB}$ found for a pulse from a

cosmic track in reference {3} is caused by the relatively large width (~ 4 mm) of the laser beam.

5. Tolerances

The many measurements done showed an excellent reproducibility of the fitted straight line calibration. Both measurements and calculations indicate that the beam focal point may lie between infinity and -70 m to give satisfactory results.

To test the required accuracy of the ratio of beam width and diaphragm radius, calculations were done for various values of this ratio. Changes of -14, +17 and +33 percent did not lead to a significant increase of the straightness errors.

The ionisation along the beam should be as constant as possible, although a fluctuation of less than 20 percent is permitted. A decrease or increase can be compensated by modifying the beam diameter by changing the BWA focal length ratio.

Increasing the drift distance to 25 mm generally improved the straightness. In general, diffusion of the electron cloud smooths down the sometimes awkward interference pattern.

If another drift chamber with different wire configuration is used, the result may be different. However, we expect that by tuning the parameters also good alignment values can be obtained. The drift path curve is likely to be the most relevant feature.

6. Conclusion

We have demonstrated that using laser induced ionisation a drift chamber calibration line can be obtained which is straight to 10 μm over eight meters. The tolerances required for the optical settings are wide enough to permit an easy reproducibility. The interference pattern caused by the diaphragm cut off appears to play an essential role. The good correspondence with results from a computer simulation indicates that the process is well understood.

Acknowledgement

We thank Dr. W. Hoogland for his help with the editing of this text.

References

- {1} H. Anderhub, M.J. Devereux and P.G. Seiler, Nucl. Instr. and Meth. 166 (1979) 581; Nucl. Instr. and Meth. 176 (1980) 323.
- {2} H.J. Hilke, Nucl. Instr. and Meth. 174 (1980) 145.
- {3} Jan Konijn and Fred Hartjes, Nucl. Instr. and Meth. 217 (1983) 311.
- {4} Svelto: Principles of Lasers, Chapter 8.2; ISBN 0-306-40862-7, Plenum.
- {5} L3 technical proposal May 1983.
- {6} J. Bourotte and B. Sadoulet, Nucl. Instr. and Meth. 173 (1980) 463.
- {7} J.C. Guo, F.G. Hartjes and J. Konijn, Nucl. Instr. and Meth. 204 (1982) 77.
- {8} Hecht/Zajac: Optics; Addison-Wesley

Figure captions

Fig. 1. Optical set up for the straightness check of the laser beam. The beam characteristics are controlled by the beam width adapter lenses C1 and C2 and by the diaphragm D.

Fig. 2. The light path in the Nitrogen laser. The beam is focused onto the diaphragm by the telescope lenses L1 and L2. The originally line shaped beam profile is converted into a more or less round one by the cylindrical lenses CL1 and CL2.

Fig. 3. Variations in the drift time sum ($T1 + T2$) and corresponding drift distance (Y) for various optical distances from the BWA (X). The zero point of Y is arbitrary. The diaphragm is 2.2 mm, the beam is focused at 15 m, the drift distance is 15 mm, the averaged amplitude of the chamber pulse is 4.2 times the discriminator threshold voltage.

Fig. 4. The same as in fig. 3 for the new settings. The diaphragm is 3.6 mm, the beam is focused at -75 m, $V_{ch}/V_{th} = 10$. The RMS deviation from a fitted straight line corresponds to 4.5 μm (first and last point excluded).

Fig. 5. Relation between RMS deviation from a fitted straight calibration line for 10 points over 8 mm (RMS) and relative pulse amplitude (V_{ch}/V_{th}). The diaphragm is 3.6 mm, the beam is focused at infinity, the drift distance is 15 mm.

Fig. 6. Comparison of the measured and calculated drift times ($T1 + T2$) along the beam. The zero point for the calculated time is arbitrary. The diaphragm is 3.6 mm, the beam is focused at -75 m, the drift distance is 15 mm, $V_{ch}/V_{th} = 5.7$.

Fig. 7. Ionisation along the beam.

1 : measured with diaphragm 3.6 mm, $\sigma_{beam} = 1.04$ mm, focus at -75 m.

2 : idem calculated.

3 : idem calculated without diaphragm, $\sigma_{beam} = 1.0$ mm.

Fig. 8. Variation of the drift time sum ($T1 + T2$) as a function of the relative amplitude (V_{ch}/V_{th}) for drift chamber pulses. This is nothing else but a logarithmic display of the shape of the rising edge of the pulse. The distance from the BWA is 1.67 m, the drift distance is 15 mm. The slope corresponds to 43 $\mu\text{m}/\text{dB}$ for $V_{ch}/V_{th} > 3$.

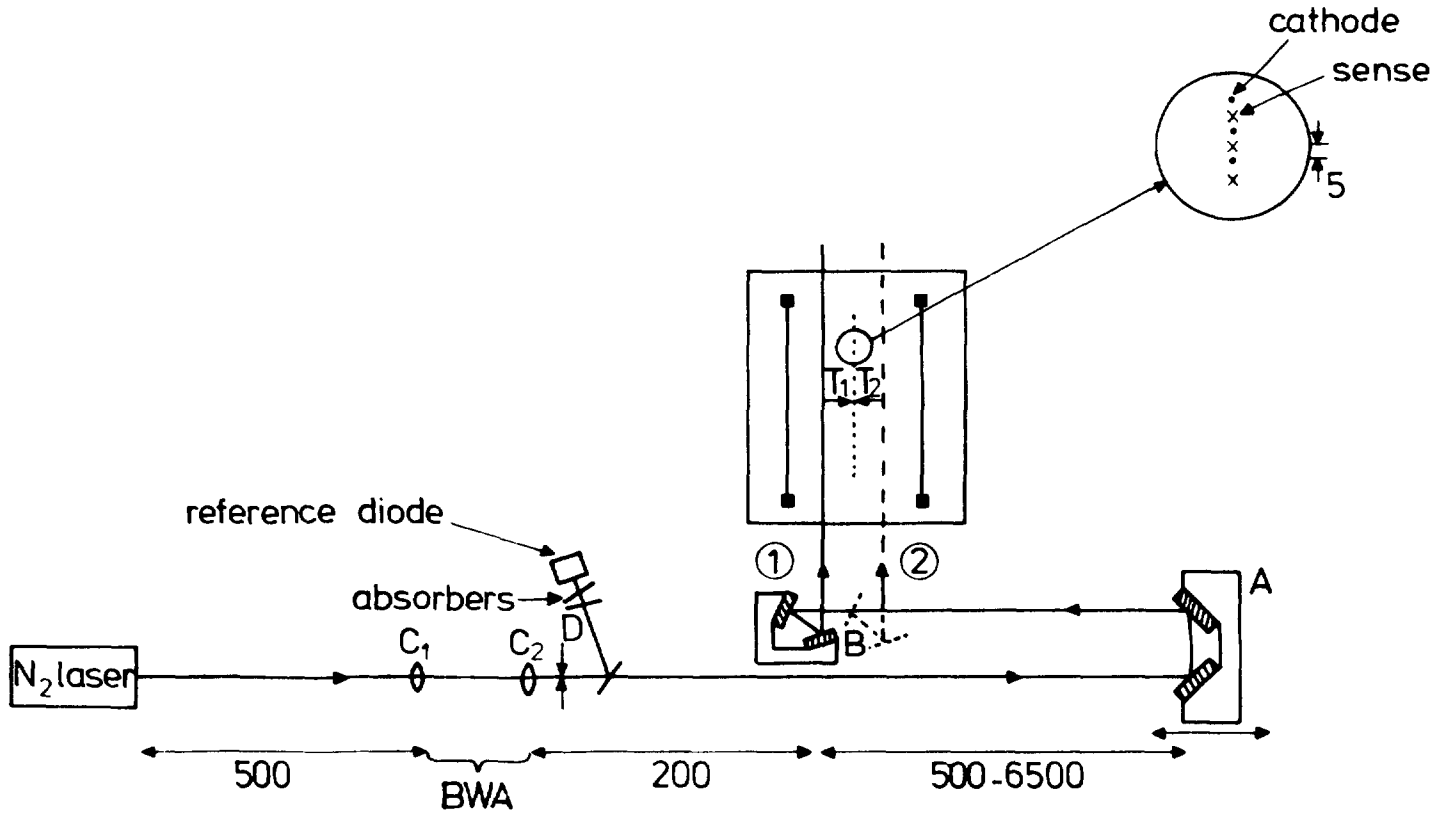


FIGURE 1.

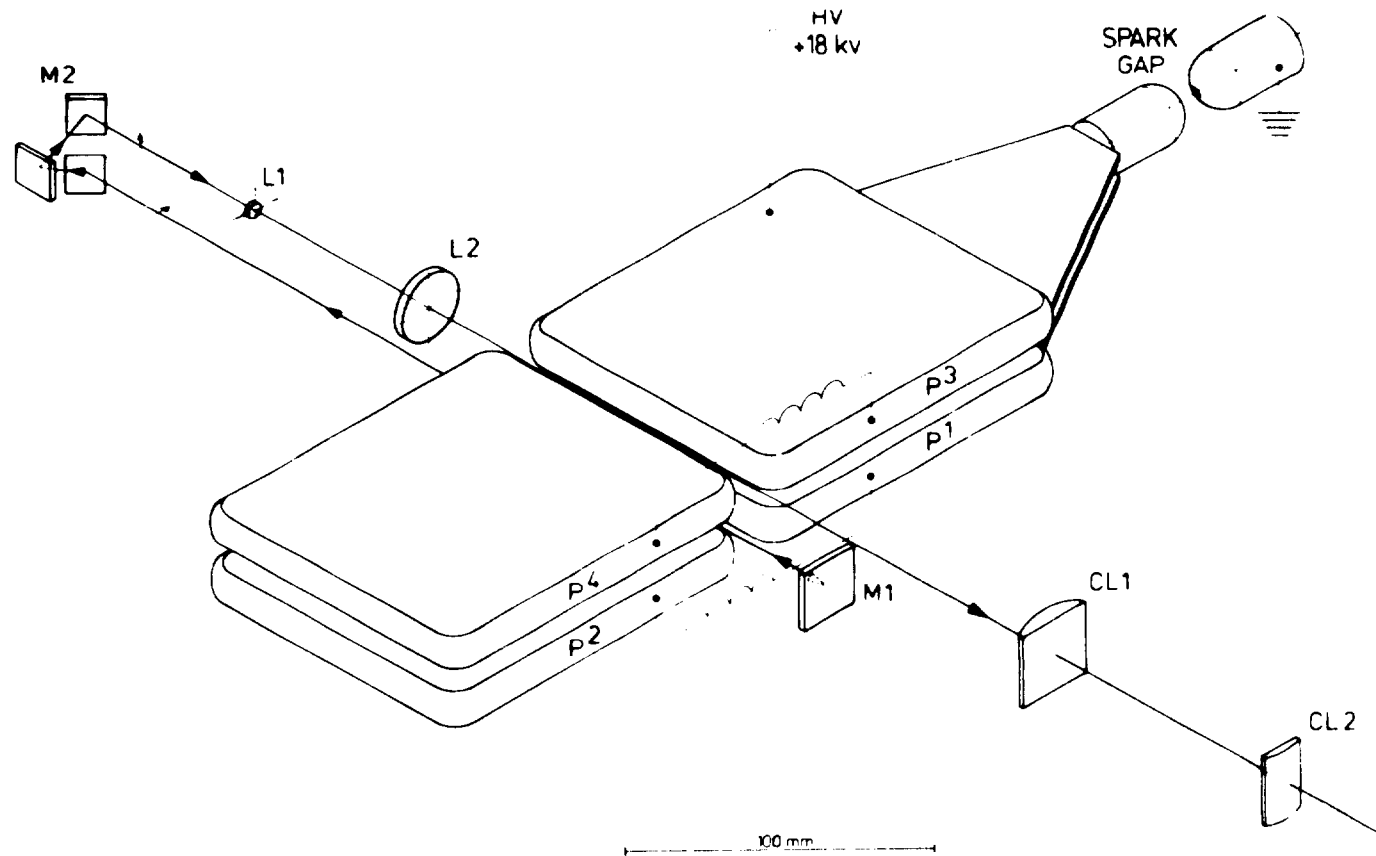


FIGURE 2.

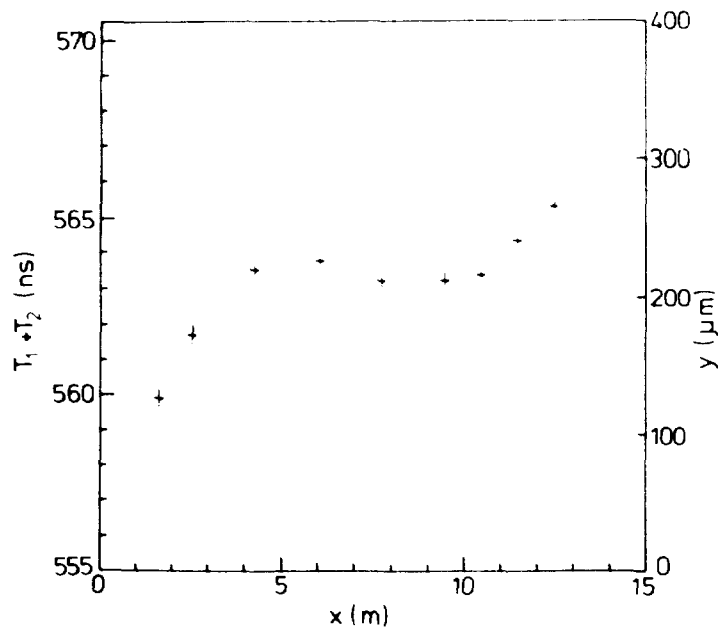


FIGURE 3.

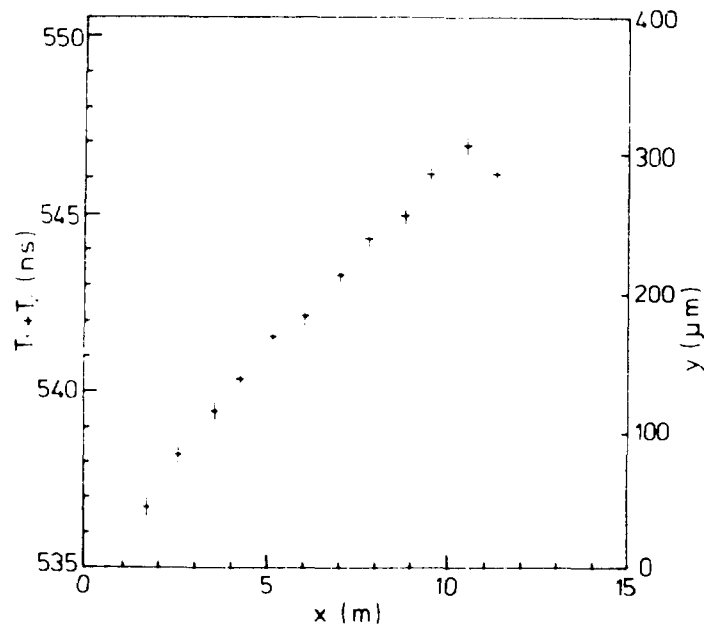


FIGURE 4.

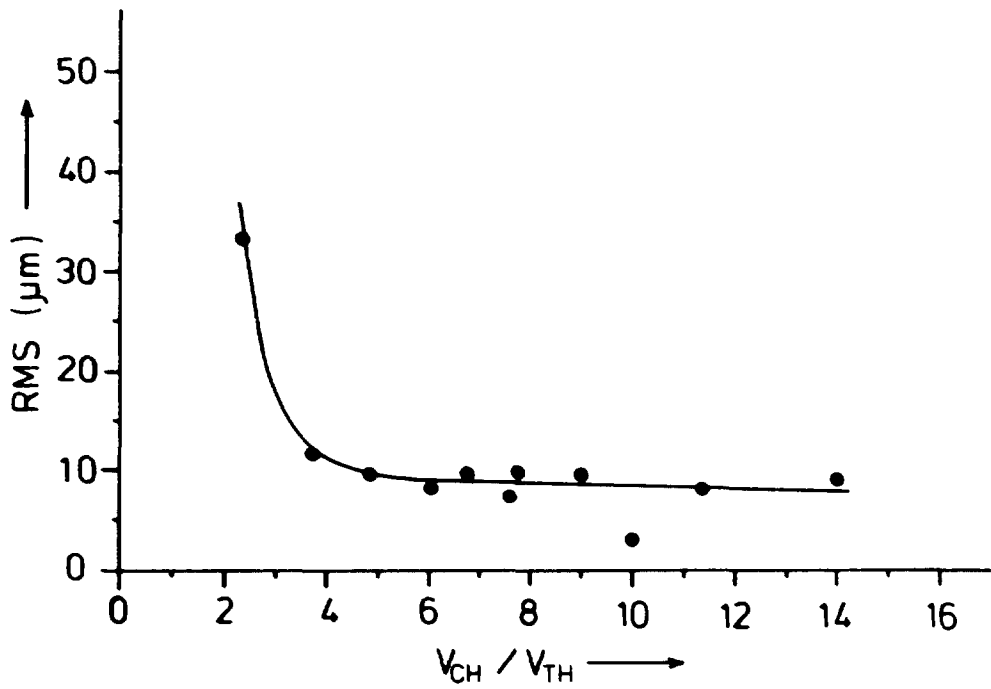


FIGURE 5.

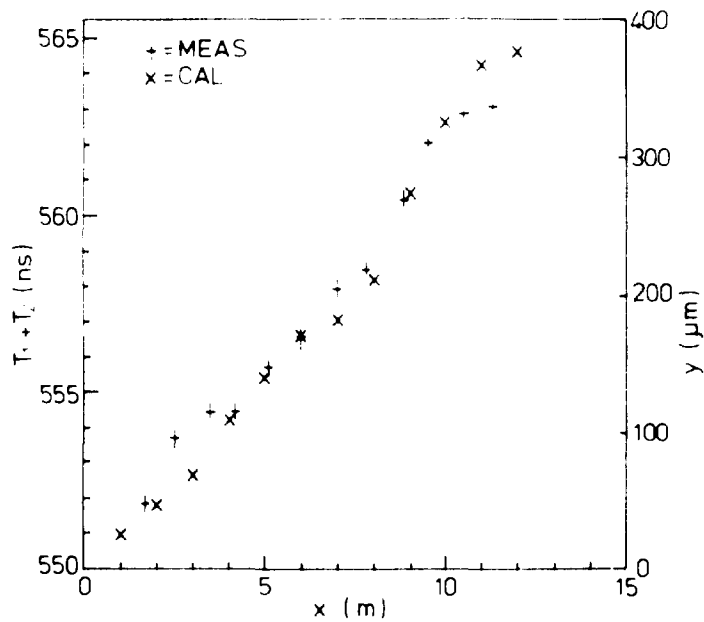


FIGURE 6.

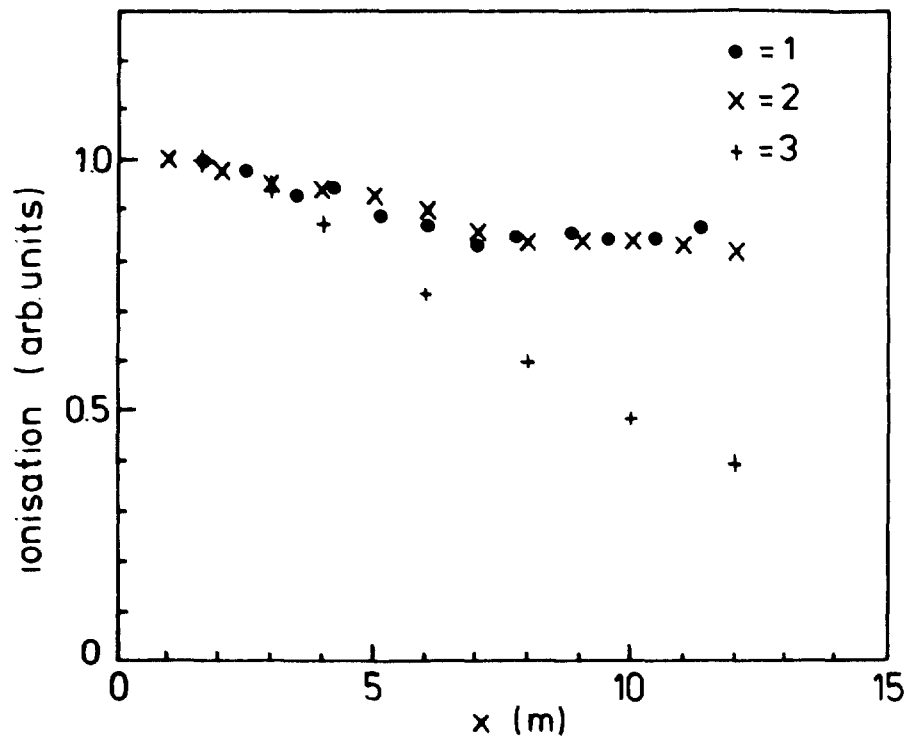


FIGURE 7.

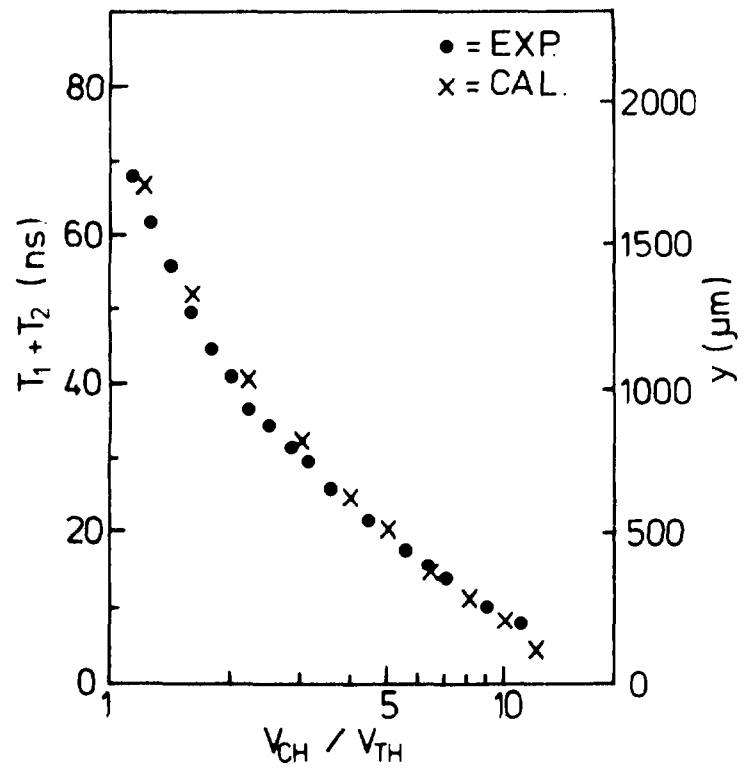


FIGURE 8.